Biochemical Pharmacology, Vol. 54, pp. 721–727, 1997.

ISSN 0006-2952/97/$17.00 + 0.00
PII S0006-2952(97)00225-6

Alendronate Inhibition of Protein-Tyrosine-Phosphatase-Meg1

Evan E. Opas,† Su Jane Rutledge,* Ellis Golub,‡ Andrew Stern,§ Zoran Zimolo,*‖ Gideon A. Rodan* and Azriel Schmidt**

*Departments of Bone Biology and Osteoporosis Research and §Pharmacology, Merck Research Laboratories, West Point, PA 19486; and ‡Department of Biochemistry, University of Pennsylvania School of Dental Medicine, Philadelphia, PA 19104, U.S.A.

ABSTRACT. Alendronate (4-amino-1-hydroxybutylidene-1,1-bisphosphonate) is a potent bisphosphonate that inhibits osteoclastic bone resorption and has proven effective for the treatment of osteoporosis. Its molecular mechanism of action, however, has not been defined precisely. Here we report that alendronate is a potent inhibitor of the protein-tyrosine-phosphatase-meg1 (PTPmeg1). Two substrates were employed in this study: fluorescein diphosphate and the phosphotyrosyl peptide src-pY^{527}. With either substrate, alendronate was a slow binding inhibitor of PTPmeg1. Among the other bisphosphonates studied, alendronate was more potent and selective for PTPmeg1. The hydrolysis of fluorescein diphosphate by PTPε and PTPmeg1 was sensitive to alendronate, with IC_{50} values of less than 1 μM; PTPσ, however, under the same conditions, was inhibited by only 50% with 141 μM alendronate. Similarly, with the src-pY^{527} substrate, alendronate inhibition was also PTP dependent. Alendronate inhibited PTPmeg1 with an IC_{50} value of 23 μM, PTPσ with an IC_{50} value of 2 μM, and did not inhibit PTPε at concentrations up to 1 mM. The alendronate inhibition of these three PTPs and two substrates is consistent with the formation of a ternary complex comprised of enzyme, substrate, and inhibitor. PTP inhibition by bisphosphonates or vanadate was diminished by the metal chelating agent EDTA, or by the reducing agent dithiothreitol, suggesting that a metal ion and the oxidation of a cysteine residue are required for full inhibition. These observations show substrate- and enzyme-specific PTP inhibition by alendronate and support the possibility that a certain PTP(s) may be the molecular target for alendronate action. BIOCHEM PHARMACOL **54**;6:721–727, 1997. © 1997 Elsevier Science Inc.

KEY WORDS. protein-tyrosine-phosphatase; bisphosphonate; alendronate; osteoporosis

BPs¶ are synthetic analogs of pyrophosphate in which a carbon atom substitutes for the oxygen that links the two phosphate groups. Addition of side chains to the carbon yields various compounds that inhibit osteoclastic bone resorption both *in vivo* and *in vitro*, providing a series of therapeutic agents with varied potency for the treatment of bone disorders such as osteoporosis, hypercalcemia of malignancy, and Paget's disease [1–4].

Osteoclasts are multinucleated cells that resorb bone at sites of bone remodeling. Protein tyrosine kinase activity seems to be essential for osteoclast function since herbimycin A, a protein-tyrosine-kinase inhibitor, and orthovanadate, a PTP inhibitor, have both been shown to inhibit bone resorption [5, 6]; moreover, the c-*src* gene knockout by homologous recombination in mice also results in inactive osteoclasts and the development of osteoporosis [7]. These osteoclasts lack ruffled borders, which are the specialized membranes in the osteoclasts, characteristic of active bone resorption [8]. This lack of ruffled border was also observed in osteoclasts from ALN-treated animals [9].

BPs, in view of their resemblance to pyrophosphate, may affect fundamental phosphate-related biochemical pathways. Protein kinases and phosphatases play pivotal roles in many cellular events including regulation of cytoskeletal functions involved in cell shape change, migration, cell fusion, and vesicular traffic [10, 11]. PTPD1, which belongs to a family of intracellular PTPs that includes PTPmeg1 and PTPH1, has been found to associate with c-*src* kinase [12]. This group of PTPs is characterized by a single catalytic domain and a region with homology to cytoskeleton-associated ezrin protein [13, 14]. We previously reported that ALN inhibits the activity of PTPε [6] and PTPσ [15]. To study further the effects of BPs on another member of the PTP family, we characterized the inhibition of PTPmeg1, and compared its effects with those on PTPε and PTPσ. We report here that ALN is a potent inhibitor of PTPmeg1 using both peptide and nonpeptide substrates.

† Corresponding author: Evan E. Opas, WP26A-1000, Department of Bone Biology and Osteoporosis Research, Merck Research Laboratories, West Point, PA 19486. Tel. (215) 652-3397; FAX (215) 652-4328; E-mail: opas@merck.com

‖ Present address: Yale University, New Haven, CT.

¶ *Abbreviations:* ALN, alendronate; BP, bisphosphonate; DTT, dithiothreitol; FDP, fluorescein diphosphate; GST, glutathione *S*-transferase; and PTP, protein-tyrosine-phosphatase.

Received 20 February 1997; accepted 15 April 1997.

MATERIALS AND METHODS

Materials

The cDNA coding for the catalytic domain of PTPmeg1 (amino acid residues 423–926) was derived from the human osteosarcoma cell line Saos-2/B10 [16] and was found to be identical to the previously described sequence [13]. PTPσ and PTPϵ were purified as GST fusion proteins as described [6, 15]. FDP and fluorescein were from Molecular Probes (Eugene, OR). The phosphopeptide TSTEPQpYQPGENL, (src-pY^{527}) was from California Peptide Research (Napa, CA). BPs were synthesized at Merck Research Laboratories (West Point, PA) or Gentili Laboratories (Pisa, Italy): ALN (4-amino-1-hydroxybutylidene-1,1-bisphosphonate); etidronate (1-hydroxyethylidene-1,1-bisphosphonate); pamidronate (3-amino-1-hydroxypropylidene-1,1-bisphosphonate); clodronate (dichloromethylene-bisphosphonate); and YM175 (cycloheptylaminomethylene-1,1-bisphosphonate). Other reagents were purchased from the Sigma Chemical Co. (St. Louis, MO).

Purification of PTPmeg1

The cDNA coding for the catalytic domain of PTPmeg1 was inserted in-frame into the bacterial expression vector pGEX-2TX (Pharmacia, Piscataway, NJ) and grown in *Escherichia coli* as a GST/PTPmeg1 fusion protein. The GST/PTPmeg1 fusion protein was isolated and purified from the bacteria according to the Pharmacia protocol. Protein concentration was determined by the method of Bradford [17]. GST/PTPmeg1 was expressed in *E. coli* with a typical yield of 0.75 mg/L. Enzyme activity and inhibition of activity by vanadate and ALN were not different when comparisons were made between the intact GST/PTPmeg1 fusion protein and the thrombin-cleaved PTPmeg1, and thus experiments utilized the GST/PTPmeg1 conjugate.

Enzyme Assays

PTPmeg1 activity with FDP as substrate was measured in a continuous assay [6] using a Millipore Cytofluor II plate reader (Bedford, MA) with an excitation wavelength of 485 nm (20 nm band width) and an emission wavelength of 530 nm (30 nm band width). The assay was performed in half volume 96-well plates (Costar, Cambridge, MA) in a buffered 100 μL solution composed of 50 mM 1,4-piperazinediethanesulfonic acid (PIPES), 0.15 M NaCl, 0.1% Tween-20, 10% glycerol, pH 6.5, at ambient temperature. Data are expressed as picomoles FDP hydrolyzed per minute per 200 ng GST/PTPmeg1, based on standard curves of fluorescence generated with fluorescein. PTPmeg1 activity with src-pY^{527} was determined by measuring the release of free phosphate by the discontinuous malachite green method [18] in a 25-μL reaction volume in a buffer consisting of 50 mM Tris, 0.15 M NaCl, 0.1% Tween-20, 10% glycerol, pH 7.9, at ambient temperature. Absorbances at 630 nm were measured after the addition of 100 μL stopping reagent in a Bio-Tek EL340 plate reader (Winooski, VT) and converted to picomoles phosphate released per 400 ng GST/PTPmeg1, based on phosphate standard curves.

Kinetic analysis of the data was carried out using the method of Duggleby for estimating the initial velocity (v_0) by fitting the progress curves to a form of the integrated rate equation:

$$t = \frac{P}{v_0} + \frac{2v_0t_{1/2} - P_\infty}{v_0(1 - \ln 4)} \cdot \left[\frac{P}{P_\infty} + \ln\left(1 - \frac{P}{P_\infty}\right)\right] \quad (1)$$

where P is the accumulated product formed at time, t, P_∞ is the final amount of product formed, and $t_{1/2}$ is the time for P to equal $P_\infty/2$ [19]. The main advantage of this robust method is that it yields reliable estimates of v_0 for a wide variety of conditions. When applied to the present data, the non-linear curve fits were well-behaved and resulted in unique parameter values. Further, this method is not perturbed by loss of reactivity resulting from enzyme lability during the reaction. Moreover, the derived parameter, v_0 can be analyzed further by standard methods of enzyme kinetics. The kinetic constants K_m and V_{max} were determined by analysis of the substrate concentration dependence of v_0. Non-linear regression was performed using the computer program, SigmaPlot (Jandel Scientific, San Rafael, CA). Inhibitor IC_{50} values were determined for the specified conditions.

Experiments with inhibitors were performed at the optimum pH and at K_m concentrations for the specific substrate. The buffer used for PTPσ was 50 mM PIPES, 0.15 M NaCl, 0.1% Tween-20, 10% glycerol, pH 6.5. For PTPϵ, inhibitor studies were performed in 50 mM 2-[*N*-morpholino]ethanesulfonic acid (MES), 0.15 M NaCl, 0.1% Tween-20, 10% glycerol, pH 5.8.

RESULTS

Characterization of PTPmeg1 Activity Using FDP and src-pY^{527} Substrates

PTPmeg1 hydrolyzed the two substrates with different pH optima (Fig. 1). Maximal hydrolysis of FDP occurred at pH 6.8, while the optimal phosphate hydrolysis from src-pY^{527} was at pH 7.9. PTPmeg1 exhibited different kinetic parameters for the two substrates. As shown in Table 1, the enzyme had a K_m of 2.0 μM for FDP and 33.0 μM for the src-pY^{527} peptide. However, PTPmeg1 had a V_{max} of 8075 pmol min^{-1} μg^{-1} with the src-pY^{527} peptide compared to a lower V_{max} of 31.9 pmol min^{-1} μg^{-1} with FDP. Substrate selectivity was demonstrated by the fact that the threonine-phosphorylated peptide, KRpTIRR, at a concentration of 200 μM, was not hydrolyzed by PTPmeg1 over a wide pH range (data not shown). PTPmeg1 activity, with both FDP and src-pY^{527}, increased linearly with protein concentration. Addition of the metal ions magnesium, calcium, and zinc (1 mM, chloride salts) had no effect on enzymatic activity.

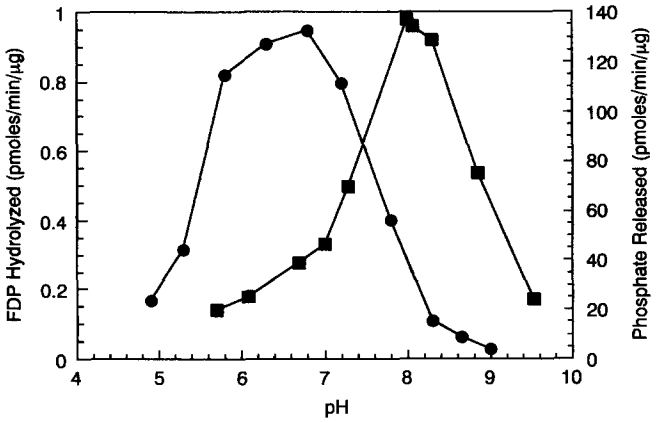

FIG. 1. Substrate specific pH optima for PTPmeg1 activity. The substrates used were 5 μM FDP (●) and 130 μM src-pY^{527} (■). Solutions of 0.15 M NaCl, 0.1% Tween-20, 10% glycerol were buffered with a 50 mM concentration of either sodium acetate, MES, HEPES, or ethanolamine. The data represent one of two experiments with the same results.

Inhibition of PTPmeg1 Activity by ALN

The dephosphorylation of both FDP (Fig. 2A) and src-pY^{527} (Fig. 2B) by PTPmeg1 was inhibited by ALN in both a concentration- and time-dependent manner. Under the conditions tested, the initial velocities of FDP hydrolysis by PTPmeg1 diminished with increasing ALN concentrations but there was no detectable effect on the apparent K_m for FDP, ~2.0 μM (Fig. 3A). In addition, the plot of initial velocities versus FDP concentration yielded curves that did not converge (Fig. 3A), consistent with noncompetitive inhibition. This was less clear for ALN inhibition of PTPmeg1 dephosphorylation of src-pY^{527}, which appeared to be competitive since the rates seemed to converge as the substrate concentration increased (Fig. 3B).

PTP inhibition by ALN was time dependent. Inhibition increased with reaction time, and the time required for maximal inhibition was inversely related to ALN concentration (Fig. 4). When ALN was preincubated with enzyme, a 1-hr preincubation with 1 μM ALN increased inhibition measured 40 min after the addition of FDP from 20 to 80%. At higher concentrations (10 μM), ALN caused 100% inhibition of the enzyme (data not shown). When the rates of inactivation were analyzed as a function of ALN concentration present during preincubation, a saturable concentration dependence was observed. The maximum velocity of this inactivation was 0.077 pmol μg^{-1} protein min^{-2}, an ALN concentration of 0.3 μM producing a half-maximal rate of inactivation (Fig. 5). The ALN inhibition of PTPmeg1 appeared irreversible upon dilution after enzyme and inhibitor were preincubated together (data not shown).

TABLE 1. Kinetic constants for PTPmeg1

Substrate	K_m (μM)	V_{max} (pmol min^{-1} μg^{-1})
FDP	2.0	31.9
src-pY^{527}	33.0	8075.0

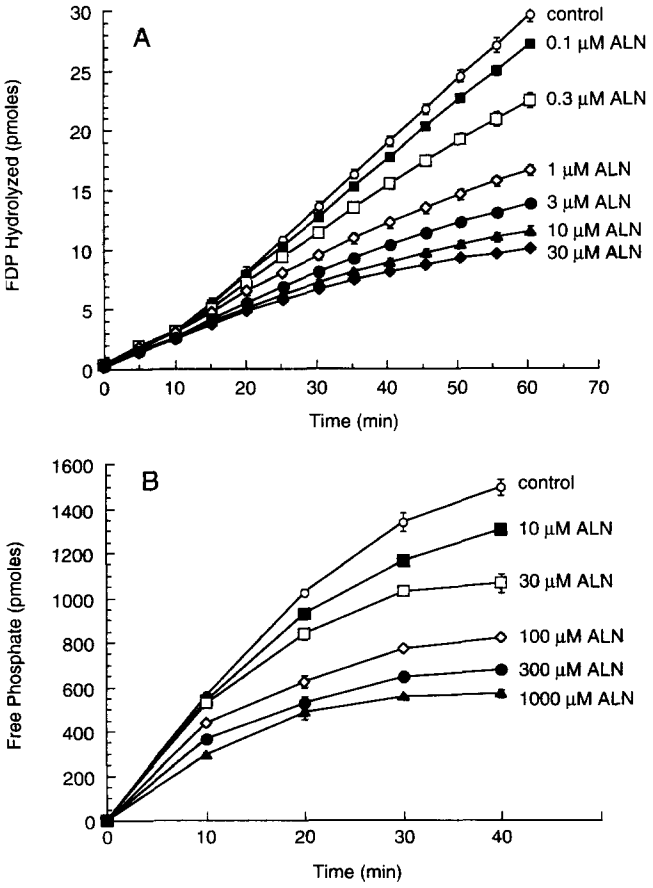

FIG. 2. PTPmeg1 activity and ALN inhibition over time. (A) FDP (5 μM) activity and ALN inhibition in a competitive reaction with 200 ng GST/PTPmeg1 in the continuous fluorescent assay described in Materials and Methods. (B) src-pY^{527} (80 μM) activity and ALN inhibition in a competitive reaction with 400 ng GST/PTPmeg1 in the discontinuous assay described in Materials and Methods. Data represent average values ± SD from 3 samples.

A requirement of PTPmeg1 for a metal to maximize ALN binding was suggested by the ability of EDTA to modulate ALN inhibition (Fig. 6). In the presence of increasing concentrations of EDTA, the ability of ALN to inhibit PTPmeg1 hydrolysis of FDP was diminished greatly. The same phenomenon was observed with vanadate. The reducing agent, DTT, can similarly shift the inhibition curves of ALN or vanadate, but not to the same extent as EDTA (Fig. 6). ALN inhibition of PTPmeg1 hydrolysis of src-pY^{527} was affected by EDTA and DTT in a similar manner (data not shown).

Substrate-Specific Inhibition of PTPmeg1 by BPs

BPs have different side chains on the central carbon connecting the two phosphate moieties, and vary greatly in their potency of inhibiting bone resorption *in vivo*. Since ALN inhibition is time dependent, we compared the

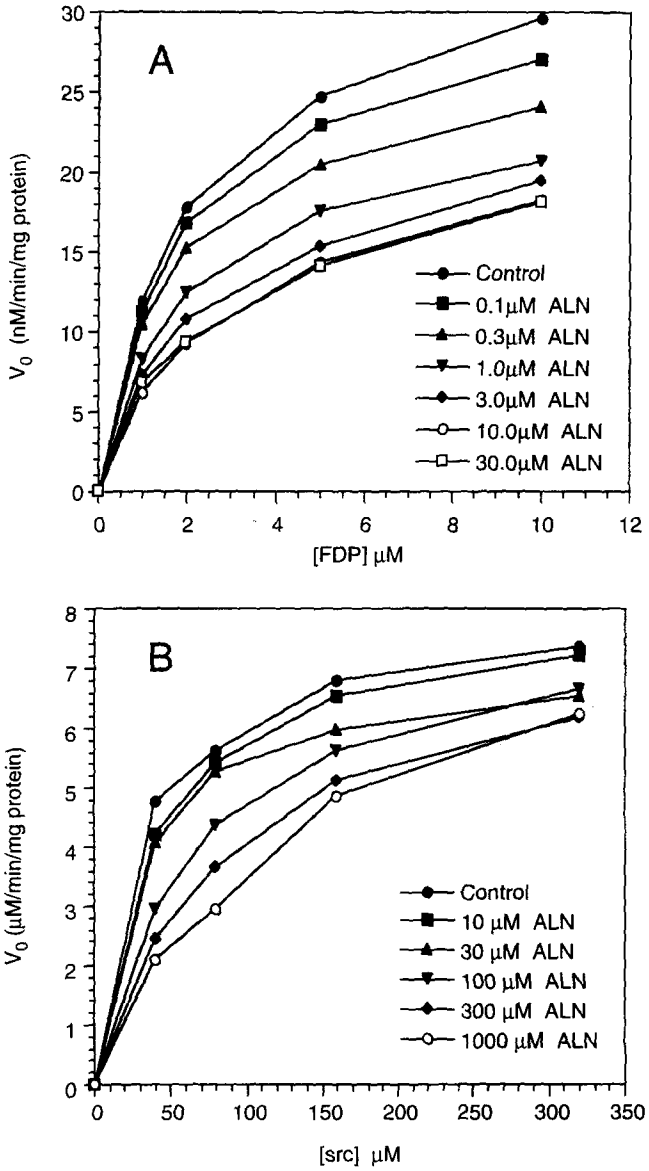

FIG. 3. Initial velocity kinetics of ALN inhibition of PTPmeg1 activities. (A) Inhibition by ALN of FDP hydrolysis. Initial velocities were derived from data depicted in Fig. 2A by the method of Duggleby [19] as described in Materials and Methods. (B) Inhibition by ALN of src-pY^{527} hydrolysis. Initial velocities were derived from data depicted in Fig. 2B by the method of Duggleby as described in Materials and Methods.

various BPs under similar conditions following preincubation with the enzyme for 15–30 min before substrate addition. When FDP was used as substrate, five distinct BPs exhibited relatively equal ability to inhibit PTPmeg1: IC_{50} values were in the range of 0.6 to 1.1 μM (Table 2). When PTPmeg1 was assayed with the src-pY^{527} substrate, distinct differences amongst the BPs were observed. ALN, etidronate, and pamidronate inhibited src-pY^{527} phosphate hydrolysis with IC_{50} values of 23, 25, and 23 μM, respectively (Table 2), whereas clodronate and YM175 inhibited the dephosphorylation of src-pY^{527} peptide with IC_{50} values of 363 and 412 μM, respectively. Vanadate inhibited PTP-

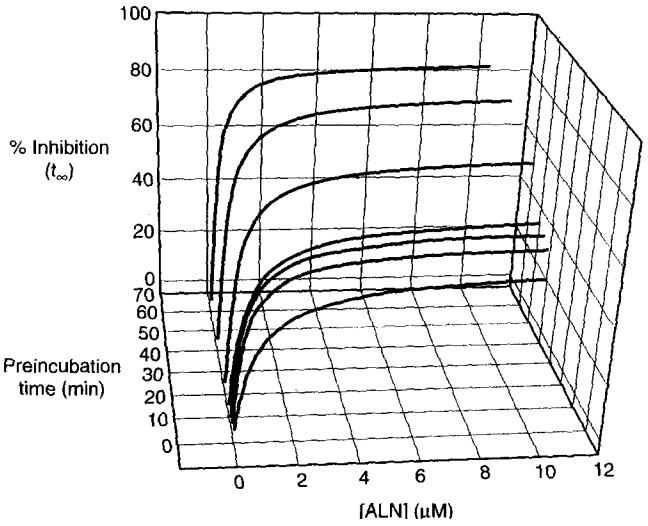

FIG. 4. Effect of preincubation on ALN inhibition of PTPmeg1. Reactions containing PTPmeg1 and substrate (FDP) were incubated in the presence of 0, 0.1, 1.0, and 10.0 μM ALN. The ALN was added 0, 2, 5, 10, 20, 40, and 60 min prior to the addition of the FDP. The production of fluorescent product was followed as a function of time for 127 min after the addition of FDP. Each time curve was evaluated as described in Materials and Methods. The computed plateau value, P, for each curve was used to compute the percent inhibition relative to the control (0 ALN) value. The percent inhibition as a function of ALN concentration was analyzed and found to obey simple saturation kinetics. The idealized curves in the figure are computed from the I_{50} and I_{max} values.

meg1 activity with an IC_{50} of 2 nM for FDP hydrolysis and 17 nM for src-pY^{527} dephosphorylation. Product inhibition was observed at millimolar concentrations of sodium phosphate, which inhibited the PTPmeg1 hydrolysis of FDP with an IC_{50} value of 6 mM.

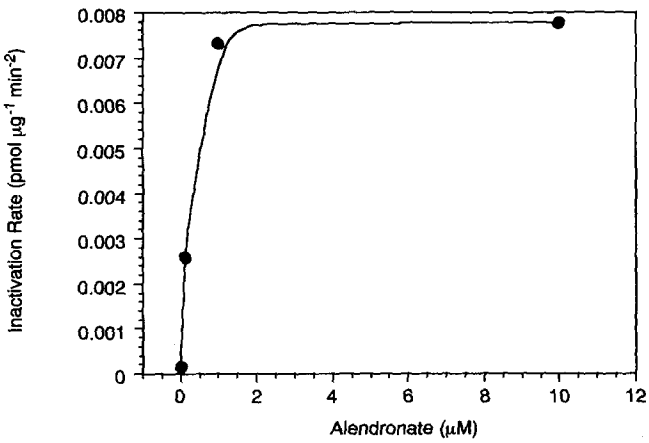

FIG. 5. Rate of inhibition of FDP hydrolysis by ALN. GST/PTPmeg1 (200 ng) was preincubated with 0, 0.1, 1.0, and 10.0 μM ALN under ambient conditions prior to the addition of 5 μM FDP. Initial velocities (v_0) were estimated according to the equation of Duggleby [19] as described in Materials and Methods. This saturation curve was generated from the slopes of the resultant rate lines versus the ALN concentration used to derive those lines. Data represent the mean values from 3 samples.

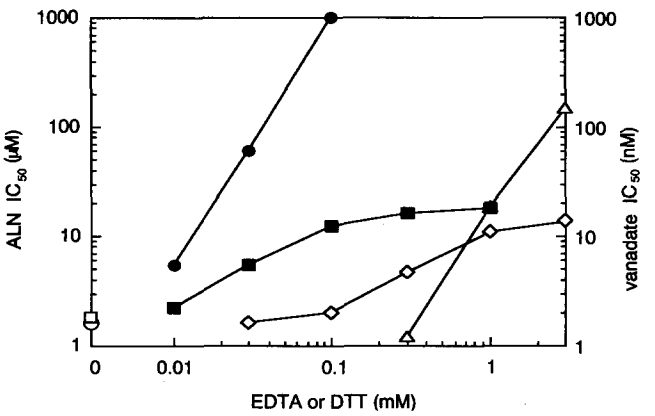

FIG. 6. Effects of EDTA and DTT on ALN and vanadate inhibition of PTPmeg1. ALN and vanadate inhibition (IC_{50} values at 30 min) of PTPmeg1 (200 ng) hydrolysis of FDP (3 μM) in a reaction in the presence or absence of various concentrations of EDTA or DTT was measured. Symbols depict the following IC_{50} values: ALN alone (○); ALN plus EDTA (●); ALN plus DTT (△); vanadate alone (□); vanadate plus EDTA (■); and vanadate plus DTT (◇). The data depicted are from one of three separate experiments with the same results.

Enzyme and Substrate-Dependent Inhibition by ALN

To study the specificity for ALN inhibition of PTPs, we compared the effects of ALN on phosphate hydrolysis by PTPσ, PTPε, and PTPmeg1. When tested with FDP as substrate, PTPmeg1 and PTPε were inhibited by ALN with IC_{50} values of 0.3 and 0.4 μM, respectively (Table 3). PTPσ, however, was relatively insensitive to ALN, exhibiting an IC_{50} value of 141 μM. When src-pY^{527} peptide was used as substrate, ALN inhibition was also strongly enzyme dependent. PTPσ and PTPmeg1 were inhibited with IC_{50} values of 2.0 and 23 μM, respectively, while ALN did not inhibit PTPε at concentrations up to 1 mM.

Vanadate is a potent inhibitor of the three PTPs in this study with either substrate. PTPmeg1 and PTPε hydrolysis of FDP was more sensitive to vanadate with IC_{50} values of 0.002 μM compared with an IC_{50} value of 0.03 μM for PTPσ. With src-pY^{527} peptide as substrate, vanadate inhibition of the PTPs exhibited IC_{50} values equal to 0.017, 0.001, and 0.03 μM for PTPmeg1, PTPσ, and PTPε, respectively.

TABLE 2. BP inhibition of PTPmeg1

	IC_{50} (μM)	
	FDP	src-pY^{527}
ALN	0.6	23
Clodronate	0.6	363
Etidronate	0.8	25
Pamidronate	0.7	23
YM175	1.1	412
Vanadate	0.002	0.017

Data are expressed as IC_{50} values relative to control activity. For FDP, this followed a 30-min preincubation of enzyme and inhibitor, and a 40-min reaction with 3 μM FDP. For src-pY^{527}, enzyme and inhibitor were preincubated for 15 min. Substrate (80 μM) was added, and the reaction proceeded for 30 min.

TABLE 3. Summary of ALN and vanadate inhibition of PTPmeg1, PTPσ, and PTPε

	IC_{50} (μM)		
	PTPmeg1	PTPσ	PTPε
With FDP			
ALN	0.26	141	0.40
Vanadate	0.002	0.03	0.002
With src-pY^{527}			
ALN	23	2.0	> 1000
Vanadate	0.017	0.001	0.03

Data represent the IC_{50} values derived from experiments in which 37 nM PTP was incubated with inhibitor for 1 hr prior to the addition of substrate (FDP or src-pY^{527}) at K_m concentrations. The reaction was then terminated after 30 min.

DISCUSSION

BPs have been documented to exert numerous biochemical effects [20–25], but except for the PTP effects reported here there have been only two previous reports of direct enzyme inhibition. Amin and his colleagues [26] have shown that BPs are potent inhibitors of squalene synthase and sterol biosynthesis. Shinozaki *et al.* [27] have shown the inhibition of bovine intestinal alkaline phosphatase hydrolysis of amino acid phosphates by pamidronate and etidronate. Recently, we showed that ALN inhibits the activity of PTPε and PTPσ using FDP as substrate [6, 15]. In this report, we further characterized the inhibition of PTP activity and demonstrated that ALN and related BPs are potent inhibitors of several protein tyrosine phosphatases, and that these BP effects can be differentiated as a function of enzyme and substrate.

Kinetic analysis suggests that, under the conditions tested here, the mode of ALN inhibition of PTPmeg1 is substrate dependent. With the relatively small non-peptide substrate FDP, ALN behaved like a noncompetitive inhibitor, while with the peptide substrate src-pY^{527}, ALN resembled a competitive inhibitor. These results are consistent with a model in which ALN binds to a site on PTPmeg1 within an extended region of the active site where it can either form a relatively tight ternary complex with enzyme and FDP or compete with src-pY^{527} for binding to free enzyme. The interaction with an extended region of the active site has been reported with other tyrosine phosphatases with macromolecules as substrates [28]. In the case of PTPmeg1, this is reflected in a comparison between the V_{max}/K_m values for the two substrates. The V_{max}/K_m value for src-pY^{527} was approximately 15-fold greater than for FDP, while the V_{max} for src-pY^{527} was approximately 250-fold greater than that for FDP. These results indicate that the intrinsic binding energy (V_{max}/K_m) of a "good substrate" is not only realized by tight binding (low K_m values) but also by an increase in V_{max}. Interactions at an extended region of the active site of PTPmeg1 could be a mechanism by which ALN forms relatively tight nonproductive complexes.

ALN inhibited PTPmeg1 activity with either substrate in this study. With FDP, PTPmeg1 and PTPε were equally

sensitive to ALN with low IC_{50} values, while PTPσ was less sensitive with an IC_{50} value of 141 μM. When src-pY^{527} was used as substrate, ALN inhibited PTPmeg1 with an IC_{50} value of 23 μM, PTPσ with an IC_{50} value of 2 μM, and did not inhibit PTPϵ, even at 1 mM ALN. The different potencies of inhibition by ALN of these three PTPs with two substrates support a model of ALN inhibition via formation of a ternary complex. Substrate-specific sensitivity to vanadate has also been observed with the PTP SHP1 [29]. Limited tryptic digestion of SHP1 resulted in both increased activity of SHP1 and increased sensitivity of peptide substrate hydrolysis to vanadate inhibition. Our observations suggest that although the catalytic domains of the PTPs are relatively similar in structure, substrate-specific inhibitors could be developed for these enzymes. Therefore, the identification of specific cellular substrates for individual PTPs could have pharmacological applications.

FDP interacts with PTPmeg1 differently than does src-pY^{527}, probably reflecting differences in the chemical structure of the two substrates. A different mode of substrate interaction was also indicated by the observation that FDP was not readily displaced by the subsequent addition of src-pY^{527} (data not shown). One cannot exclude the possibility that the different assay conditions (pH) used with the two substrates may account for the differences in ALN inhibition of PTPmeg1. However, the differences in ALN inhibition, reflected in IC_{50} values, were even more pronounced between the two enzymes PTPσ and PTPϵ (Table 3), when either substrate was used at its pH optimum, thus under identical assay conditions.

The ability of the metal chelator EDTA to modulate ALN and vanadate inhibition suggests the possibility that a metal is involved in the inhibitory complexes. Additionally, the negative shift in ALN and vanadate potency in the presence of DTT suggests that the oxidation state of a cysteine residue, perhaps in the active site of PTPmeg1, may be of critical importance in realizing full ALN or vanadate inhibition.

The various BPs tested inhibited the dephosphorylation of FDP by PTPmeg1 with similar potencies; however, with the src-pY^{527} peptide as substrate, clodronate and YM175 showed lower inhibitory activity as compared with ALN, etidronate, or pamidronate. It is possible that clodronate and YM175, with their chlorine and ring moieties, respectively, are not as accessible to the enzyme when competing with the peptide substrate. This substrate selectivity that separated the tested BPs into two groups, based on their ability to inhibit a particular enzyme/substrate combination, raises the possibility that another substrate and/or PTP, the putative BP target, could show inhibitor selectivity, consistent with the potency differences observed among BPs.

It has been shown that ALN incorporates rapidly and specifically into bone [30], where it localizes preferentially on bone resorptive surfaces and can reach 100 μM or more in resorption lacunae [9, 31]. Furthermore, ALN is internalized and concentrated within the osteoclast [9, 31]. Thus, ALN at therapeutic doses could achieve a sufficient concentration to inhibit PTP(s) within the osteoclast. Secondary exposure of osteoblasts to BPs may also occur as they can exist in close proximity to osteoclasts. Conditioned media from osteoblasts treated *in vitro* with BPs have been reported to affect osteoclast activity [22]. Osteoblasts, with perhaps their own specific PTPs, may respond in a different manner to BP than osteoclasts [15].

PTPmeg1 is not necessarily the PTP that is inhibited in osteoclasts by ALN. To identify the particular PTP that is responsible for the inhibition of osteoclast activity by BPs, one must isolate and characterize all the PTPs expressed in bone and test their activities with various BPs. It is possible that even with the relevant PTP and endogenous substrate identified, the therapeutic ratio between BPs may not be reflected by the results of an *in vitro* enzyme assay. One must also take into account that the relative *in vivo* potencies exhibited by the various BPs may stem from the cumulative effects of pharmacodynamic and pharmacokinetic parameters (e.g. differential adsorption to skeletal hydroxyapatite) as well.

In conclusion, we have demonstrated that BPs can inhibit the *in vitro* activity of PTPs in a substrate- and enzyme-dependent manner. Given the known importance of protein tyrosine phosphorylation for osteoclast function [6], these studies support the possibility that ALN inhibition of PTP activity plays a role in its pharmacological action.

References

1. Francis MD, Russell RGG and Fleisch H, Diphosphonates inhibit formation of calcium phosphate crystals *in vitro* and pathological calcification *in vivo*. *Science* **165:** 1264–1266, 1969.
2. Kanis JA, Gertz BJ, Singer F and Ortolani S, Rationale for the use of alendronate in osteoporosis. *Osteoporos Int* **5:** 1–13, 1995.
3. Liberman UA, Weiss SR, Broll J, Minne HW, Quan H, Bell NH, Rodriguez-Portales J, Downs RW Jr, Dequeker J, Favus M, Seeman E, Recker RR, Capizzi T, Santora AC II, Lombardi A, Shah RV, Hirsch LJ and Karpf DB, Effect of oral alendronate on bone mineral density and the incidence of fractures in postmenopausal osteoporosis. *N Engl J Med* **333:** 1437–1443, 1995.
4. Siris E, Weinstein RS, Altman R, Conte JM, Favus M, Lombardi A, Lyles K, McIlwain H, Murphy WA Jr, Reda C, Rude R, Seton M, Tiegs R, Thompson D, Tucci JR, Yates AJ and Zimering M, Comparative study of alendronate versus etidronate for the treatment of Paget's disease of bone. *J Clin Endocrinol Metab* **81:** 961–967, 1996.
5. Yoneda T, Lowe C, Lee C-H, Gutierrez G, Niewolna M, Williams PJ, Izbicka E, Uehara Y and Mundy GR, Herbimycin A, a pp60$^{c\text{-}src}$ tyrosine kinase inhibitor, inhibits osteoclastic bone resorption *in vitro* and hypercalcemia *in vivo*. *J Clin Invest* **91:** 2791–2795, 1993.
6. Schmidt A, Rutledge SJ, Endo N, Opas EE, Tanaka H, Wesolowski G, Leu C-T, Huang Z, Ramachandran C, Rodan SB and Rodan GA, Protein-tyrosine phosphatase activity regulates osteoclast formation and function: Inhibition by alendronate. *Proc Natl Acad Sci USA* **93:** 3068–3073, 1996.

7. Soriano P, Montgomery C, Geske R and Bradley A, Targeted disruption of the c-*src* proto-oncogene leads to osteopetrosis in mice. *Cell* **64:** 693–702, 1991.
8. Boyce BF, Yoneda T, Lowe C, Soriano P and Mundy GR, Requirement of $pp60^{c\text{-}src}$ expression for osteoclasts to form ruffled borders and resorb bone in mice. *J Clin Invest* **90:** 1622–1627, 1992.
9. Sato M, Grasser W, Endo N, Atkins R, Simmons H, Thompson DD, Golub E and Rodan GA, Bisphosphonate action. Alendronate localization in rat bone and effects on osteoclast ultrastructure. *J Clin Invest* **88:** 2095–2105, 1991.
10. Sun H and Tonks NK, The coordinated action of protein tyrosine phosphatases and kinases in cell signaling. *Trends Biochem Sci* **19:** 480–485, 1994.
11. Hunter T, Protein kinases and phosphatases: The yin and yang of protein phosphorylation and signaling. *Cell* **80:** 225–236, 1995.
12. Møller NPH, Møller KB, Lammers R, Kharitonenkov A, Sures I and Ullrich A, Src kinase associates with a member of a distinct subfamily of protein-tyrosine phosphatases containing an ezrin-like domain. *Proc Natl Acad Sci USA* **91:** 7477–7481, 1994.
13. Gu M, York JD, Warshawsky I and Majerus PW, Identification, cloning, and expression of a cytosolic megakaryocyte protein-tyrosine-phosphatase with sequence homology to cytoskeletal protein 4.1. *Proc Natl Acad Sci USA* **88:** 5867–5871, 1991.
14. Yang Q and Tonks NK, Isolation of a cDNA clone encoding a human protein-tyrosine phosphatase with homology to the cytoskeletal-associated proteins band 4.1, ezrin, and talin. *Proc Natl Acad Sci USA* **88:** 5949–5953, 1991.
15. Endo N, Rutledge SJ, Opas EE, Vogel R, Rodan GA and Schmidt A, Human protein tyrosine phosphatase-σ: Alternative splicing and inhibition by bisphosphonates. *J Bone Miner Res* **11:** 535–543, 1996.
16. Rodan SB, Imai Y, Thiede MA, Wesolowski G, Thompson D, Bar-Shavit Z, Shull S, Mann K and Rodan GA, Characterization of a human osteosarcoma cell line (Saos-2) with osteoblastic properties. *Cancer Res* **47:** 4961–4966, 1987.
17. Bradford MM, A rapid and sensitive method for the quantitation of microgram quantities of protein utilizing the principle of protein-dye binding. *Anal Biochem* **72:** 248–254, 1976.
18. Harder KW, Owen P, Wong LKH, Aebersold R, Clark-Lewis I and Jirik FR, Characterization and kinetic analysis of the intracellular domain of human protein tyrosine phosphatase β (HPTPβ) using synthetic phosphopeptides. *Biochem J* **298:** 395–401, 1994.
19. Duggleby RB, Estimation of the initial velocity of enzyme-catalysed reactions by non-linear regression analysis of progress curves. *Biochem J* **228:** 55–60, 1985.
20. Fleisch H, Bisphosphonates: Mechanisms of Action and Clinical Applications. In: *Bone and Mineral Research Annual 1* (Ed. Peck WA), pp. 319–357. Excepta Medica, Amsterdam, 1983.
21. Hughes DE, Mian M, Guilland-Cumming DF and Russell RGG, The cellular mechanism of action of bisphosphonates. *Drugs Exp Clin Res* **17:** 109–114, 1991.
22. Sahni M, Guenther HL, Fleisch H, Collin P and Martin TJ, Bisphosphonates act on rat bone resorption through the mediation of osteoblasts. *J Clin Invest* **91:** 2004–2011, 1993.
23. Klein G, Martin J-B and Satre M, Methylenediphosphate, a metabolic poison in *Dictyostelium discoideum*. ^{31}P NMR evidence for accumulation of adenosine 5′-(β,γ-methyleneetriphosphate) and diadenosine $5',5'''$-P^1,P^4-(P^2,P^3-methyleneetetraphosphate). *Biochemistry* **27:** 1897–1901, 1988.
24. Tsuchimoto M, Azuma Y, Higuchi O, Sugimoto I, Hirata N, Kiyoki M and Yamamoto I, Alendronate modulates osteogenesis of human osteoblastic cells *in vitro*. *Jpn J Pharmacol* **66:** 25–33, 1994.
25. Nishikawa M, Akatsu T, Katayama Y, Yasutomo Y, Kado S, Kugai N, Yamamoto M and Nagata N, Bisphosphonates act on osteoblastic cells and inhibit osteoclast formation in mouse marrow cultures. *Bone* **18:** 9–14, 1996.
26. Amin D, Cornell SA, Gustafson SK, Needle SJ, Ulrich JW, Bilder GE and Perrone MK, Bisphosphonates used for the treatment of bone disorders inhibit squalene synthase and cholesterol biosynthesis. *J Lipid Res* **33:** 1657–1663, 1992.
27. Shinozaki T, Watanabe H, Arita S and Chigira M, Amino acid phosphatase activity of alkaline phosphatase. A possible role of protein phosphatase. *Eur J Biochem* **227:** 367–371, 1995.
28. Zhang Z-Y and Dixon JE, Protein tyrosine phosphatases: Mechanism of catalysis and substrate specificity. *Adv Enzymol Relat Areas Mol Biol* **68:** 1–36, 1994.
29. Zhao Z, Bouchard P, Diltz CD, Shen SH and Fischer EH, Purification and characterization of a protein tyrosine phosphatase containing SH2 domains. *J Biol Chem* **268:** 2816–2820, 1993.
30. Lin JH, Bisphosphonates: A review of their pharmacokinetic properties. *Bone* **18:** 75–85, 1996.
31. Masarachia P, Weinreb M, Balena R and Rodan GA, Comparison of the distribution of ^3H-alendronate and ^3H-etidronate in rat and mouse bones. *Bone* **19:** 281–290, 1996.